

2 Separation of nearby hadronic showers in the 3 CALICE SDHCAL prototype detector using 4 ArborPFA

R. Été^{a*}

^a *Université de Lyon, Université Lyon 1, CNRS/IN2P3, IPNL, 4 Rue E. Fermi, 69622
Villeurbanne Cedex, France*

5 *E-mail:* rete@ipnl.in2p3.fr

ABSTRACT:

A new reconstruction algorithm, ArborPFA, is developed to separate nearby hadronic showers in the SDHCAL prototype. This intends to demonstrate the capability of high granularity hadronic calorimeters such as the SDHCAL to efficiently apply Particle Flow Algorithms at future ILC
6 experiments. The reconstruction algorithm we present here uses the tree-like structure features of hadronic showers, that high granular calorimeters reveal, to associate clusters belonging to each hadronic shower and to reduce the confusion between two close-by showers. The results of these studies indicate a good single particle efficiency and powerful separation down to distance of 5 cm.

*Corresponding author.

8 **Contents**

9	1. Introduction	2
10	2. The SDHCAL prototype	3
11	3. The Arbor particle flow algorithm	4
12	3.1 Principle	4
13	3.2 Pre-clustering phase	5
14	3.3 The main clustering phase - Connectors and trees	6
15	3.4 Association algorithms	8
16	4. Single particle study	12
17	4.1 Setup	12
18	4.2 Single particle analysis	12
19	5. Separation of two close-by hadronic showers	15
20	5.1 Overlay procedure and setup	15
21	5.2 Overlaid particles analysis	16
22	6. Summary	19
23	A. ArborPFA algorithm parameters	21
24	B. SDHCAL data	27

26 Keywords: Particle flow; Calorimetry; ILC; SDHCAL

1. Introduction

To study the Higgs boson properties and to extend the discovery of new particles beyond the scope of LHC, a linear $e^+ e^-$ collider such as the ILC is proposed. An important requirement of such a machine is to provide a good jet energy resolution ($\Delta E/E \sim 3-4\%$) in order to distinguish between Z and W^\pm bosons as well as to study the Higgs boson properties.

The Particle Flow concept has been proposed to achieve the ILC benchmarks [2]. This algorithm aims to individually reconstruct particles using the most appropriate sub-detector for the energy and momentum measurement. An implementation of the particle flow algorithm called PandoraPFA has been developed [5] and successfully applied in ILD physics performance studies and to close-by hadronic showers separation using AHCAL beam test data

To apply efficiently the Particle Flow Algorithms, both good energy resolution and fine transverse and longitudinal segmentation should be provided by the *electromagnetic calorimeter* (ECAL) and the *hadronic calorimeter* (HCAL).

Different calorimeter technologies are currently under study by the CALICE collaboration to fulfill these requirements. In this framework, a *semi digital hadronic calorimeter* prototype (SD-HCAL) was built [1] and successfully tested at the CERN H6 test beam lines of the SPS (CERN) in 2012. With a transverse readout segmentation of 1 cm^2 , 48 sampling layers and good energy resolution [1], this calorimeter satisfies ILC requirements.

In this paper, we present an other approach of the particle flow : the ArborPFA approach. The algorithm has been designed for high granularity calorimeters and applied to SDHCAL test beam data. We propose to evaluate the performance of the algorithm on single pion events and to study the ability of the algorithm to separate two overlaid pion showers at different separation distances and energies.

2. The SDHCAL prototype

The SDHCAL prototype is a sampling calorimeter which consists of 48 layers alternating a 20 mm steel absorbers and a 6 mm gas resistive plate chamber (GRPC) with their embedded electronics. The gas gap between the two electrodes of the GRPC is 1.2 mm. 9216 pads (96 x 96) of 1cm² compose the readout of each chamber, leading to a total number of 442368 channels. Signals from particles crossing the gas gap are recorded on those pads in a 2-bits format corresponding to 3 thresholds on the induced charge. A complete description of the calorimeter setup and its features can be found in [1].

The test beam data used in this paper were taken at the CERN H6 beam line in 2012. The pion event selection is also performed according to the selection presented in [1].

The reconstructed energy of a single particle is computed as follows :

$$E_{rec} = \alpha(N_{hit}) \cdot N_1 + \beta(N_{hit}) \cdot N_2 + \gamma(N_{hit}) \cdot N_3 \quad (2.1)$$

where α , β and γ are quadratic functions of the number of hits N_{hit} and N_1 , N_2 and N_3 are the number hits of threshold 1, 2 and 3, where $N_{hit} = N_1 + N_2 + N_3$. The nine parameters of these functions are extracted from a χ^2 minimization :

$$\chi^2 = \sum_{evt} \frac{(E_{beam} - E_{rec})^2}{E_{beam}} \quad (2.2)$$

This minimization was performed over all the hadronic events in the energy range [10, 80] GeV by step of 10 GeV. The linearity and energy resolution will be shown in section 4 dedicated to the single particle study.

3. The Arbor particle flow algorithm

3.1 Principle

The Arbor approach has been developed by the ALEPH collaboration and recently adapted [7] for ILD detector design. It is based on the idea that the hadronic shower development follows a tree-like topology.

Figure 1 shows the shower development after a proton interaction (left) in which we can see the multiple components of the shower : charged particles, neutral particles, electromagnetic and hadronic parts. The same figure shows on the right a sampling calorimeter view of a shower interaction as seen in a highly granular calorimeter. The black arrows drawn on this view suggest the tree-like topology development of the shower.

With such an approach, the shower reconstruction follows a principle close to the underlying physics.

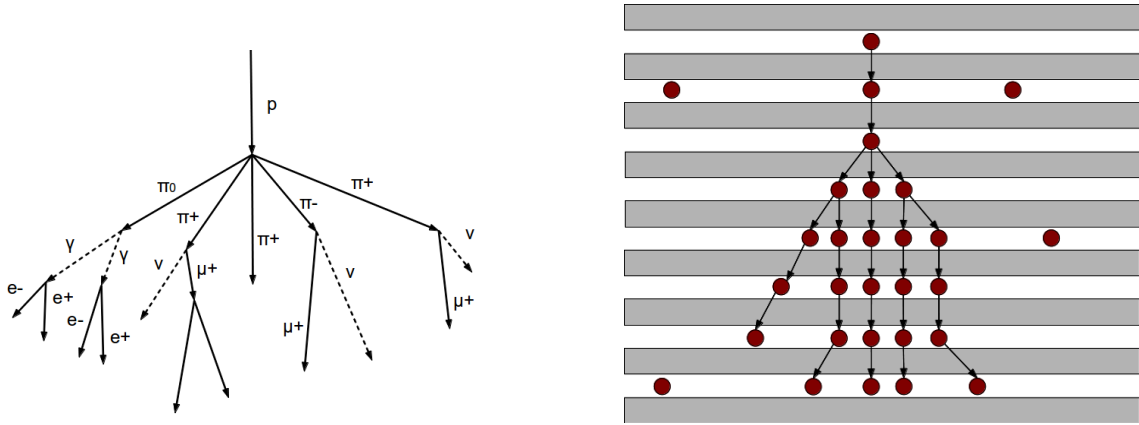


Figure 1: Left : schematic view of an induced proton shower. Right : schematic view of a reconstructed shower in a calorimeter with calorimeter hits (red)

The algorithm we present here is implemented using the PandoraSDK API as a toolkit for generic PFA development [6]. The API is used in a Marlin [4] c++ processor as part of the reconstruction chain in ILCSoft [8]. It produces only a ROOT [9] file containing the variable needed for the analysis described in this document.

Before describing the algorithm in detail, a few definitions specific to ArborPFA need to be introduced :

Object An *object* is a calorimeter hit or a group of contiguous calorimeter hits within a layer that serves as a vertex for the ArborPFA algorithm. This was introduced for two reasons i) to provide a generalization of connections between *objects* without making any assumptions of what is contained in an *object*, ii) to overcome the pad multiplicity¹ inherent in the SDHCAL [1] and similar detectors.

¹More than one pad could be fired when a particle crosses the gas gap.

90 **Flow direction** The flow direction is of two kinds : forward direction which is from upstream to
 91 downstream of the beam direction and backward direction for the opposite.

92 **Connector** A connector is a link between two *objects*. It has a weight and a direction.

93 **Connector depth** The connector depth is defined as the number of intermediary connectors link-
 94 ing two different objects.

95 **Tree** A tree is a set of *objects* connected in a tree topology, which means that for each object
 96 there is only one backward connector. An *object* without a backward connector is called a seed and
 97 an *object* without a forward connector is called a leaf.

98 **Cluster** A cluster is a set of trees.

99 **Particle flow object (PFO)** A particle flow object is a set of clusters and tracks ², which corre-
 100 sponds to a reconstructed particle.

101

102 Note that in the following algorithm descriptions, some parameters are labelled by a name or sym-
 103 bol, whose values are given in Appendix A.

104 3.2 Pre-clustering phase

105 Before building trees, we need to create objects to connect with each other.

106 **Object creation** When a particle goes through the
 107 detector, several pads can be fired in a single layer,
 108 leading to a multiplicity greater than 1. To overcome
 109 this problem, intra-layer groups of hits are assembled
 110 using the nearest neighbour clustering algorithm (cor-
 111 ner neighbours not included). If a group contains more
 112 than 4 hits, it is split and each individual hit is consid-
 113 ered as a separate object. This generally happens in
 114 the shower core. If a group contains 4 or less hits, it
 115 is used to define a single object. This is the case for a
 116 mip or more generally any isolated non-showering par-
 117 ticle. Figure 2 shows the output of this algorithm with
 118 encircled hits forming objects.

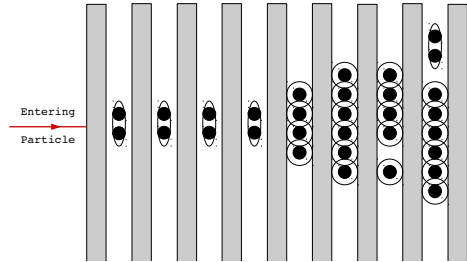


Figure 2: Schematic view of the object creation output. Small groups of contiguous calorimeter hits are grouped together (encircled).

119 **Track segment³ candidate tagging** In order to correctly reconstruct the primary track segment
 120 in the calorimeter, track segment candidate *objects* are identified and tagged for future treatment.
 121 For each object, we count the number of objects in the same layer within a distance of Δ_{mip} . If this
 122 number doesn't exceed $N_{obj,cut}$, the object is tagged as a track segment candidate object.

²By *track* we mean one reconstructed by a tracking detector such as a TPC

³By *track segment* we mean a track produced by a charged particle in the calorimeter such as Minimum Ionizing Particles (MIP)

3.3 The main clustering phase - Connectors and trees

The main clustering algorithm consists of an iterative procedure using dedicated algorithms to create and remove connectors (connector loop). At the end of this step, all objects are arranged in a tree structure, which means that each object has at most one connector in the backward direction and 0 or more in the forward direction.

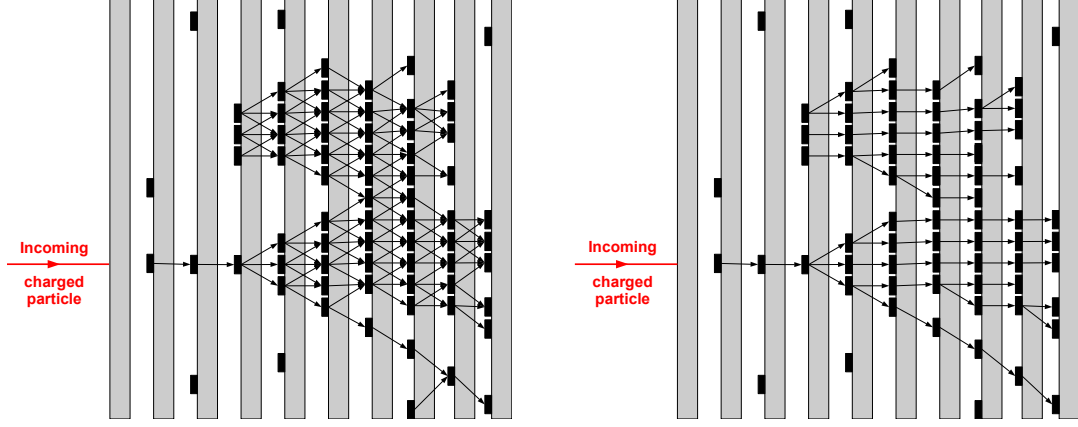


Figure 3: Schematic view of a neutral and a charged pion showers after the first connector seeding algorithm (left) and cleaning algorithm (right)

In the current implementation, the connector loop contains the following algorithms :

Primary track connection This algorithm aims to create connections between objects belonging to the primary track segment of charged particles in the calorimeter. It consists mainly in creating a sub-list of objects that are candidates for the primary track segments by using the objects tagged as track segment candidates and the track extrapolations on the front of the calorimeter. Once this list is built, the "*connector seeding 1*" algorithm and the "*connector cleaning 1*" algorithm are run on only the sub-list objects.

Connector seeding 1 We start by creating connections in the neighbourhood of each object. For each object, we look for other objects in the N_{layers} next layers within a maximum distance Δ_{max} and we create connections between them. As an example, Figure 3 (left) illustrates the output of this algorithm.

Connector cleaning 1 Once connectors are created, we need to build a tree structure by keeping only one connector in the backward direction for each object. We define the reference direction of an object as :

$$\vec{C}_{ref} = w_{bck} \cdot \sum_{\sigma} \sum_b \vec{c}_{b,\sigma} - w_{fwd} \cdot \sum_{\delta} \sum_f \vec{c}_{f,\delta} \quad (3.1)$$

where :

- w_{bck} (w_{fwd}) is a global positive weight assigned to backward (forward) connectors

- $\vec{c}_{b,\sigma}$ ($\vec{c}_{f,\delta}$) is the direction of a backward (forward) connector at the connector depth σ (δ) from the considered object

The depth parameter σ has been fixed to 1 in all algorithms. The reference direction is a vector that goes in the backward direction and indicates the most probable direction for a unique backward connection. Then we need to assign which backward connector should be kept for the tree building. Thus, for each backward connector of an object, we define the κ order parameter as :

$$\kappa = \left(\frac{\theta}{\pi}\right)^{p_\theta} \cdot \left(\frac{\Delta}{\Delta_{max}}\right)^{p_\Delta} \quad (3.2)$$

where :

- θ is the angle between a backward connector and the reference direction of the considered object,
- Δ is the distance between the connected objects,
- p_θ (p_Δ) is a power parameter for the normalized angle (distance)

The κ parameter quantifies the alignment with the reference direction within the range $[0,1]$. Smaller is this parameter, higher the alignment will be. The power parameters p_θ and p_Δ are to be tuned depending on which variable we want to emphasize.

The chosen backward connector for the tree building is the one with the smallest κ parameter; all others are removed from the list. The removal of connectors is done at the end of the algorithm so that all connectors contribute to the evaluation of the reference direction.

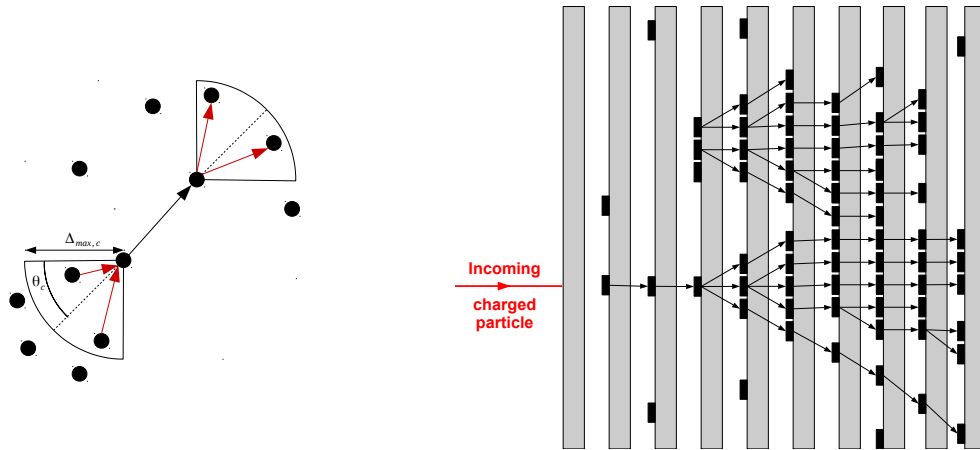


Figure 4: Left : Schematic view of the connector alignment procedure. In black, a considered connector and in red possible new connectors in backward and forward directions. Right : a neutral and a charged pion showers after the second connector cleaning algorithm

Connector seeding 2 This second step of connector seeding starts from the tree structure obtained after the first connector cleaning algorithm. The goal of this second step is to create an

alignment of connectors within the shower. For each connector, more forward connectors are created from the forward object of this connector by looking in a cone of half-angle θ_c and a maximum distance of $\Delta_{max,c}$. In the same way, additional backward connectors are created from the backward object of this connector. A schematic view of this step is shown in figure 4.

Connector cleaning 2 Here, we again need to clean up the backward connector list to end up with only one connector per object. This last algorithm is similar to the first connector cleaning except that the cleaning is done layer per layer starting from the downstream layers with a depth parameter δ strictly higher than one. For a given connector, this accentuates the alignment with the forward ones. We end up then with a tree structure again.

Tree building This step is straight-forward. Seed objects are identified and trees are built by recursively following the forward connected objects. At this step, clusters are built each containing a single tree.

The following algorithms associate some of the trees with each other.

3.4 Association algorithms

Energy driven track cluster association The track to cluster association is performed using three different pieces of information, the cluster energy, the track momentum and the cluster topology. We first look at the track projection on the calorimeter front face. Two different cases may occur :

- the particle has interacted before the calorimeter or in the first layer. In this case, many seed objects are found in the N_{layer} first layers at a maximum distance of $\Delta_{track-cluster_1}$ of the track projection. Seed objects are then sorted by their distance to the track projection. The clusters associated to their seeds are then associated to the track progressively starting from the closest one until the difference between the track momentum and the total cluster energy is minimized. The clusters are then merged since they belong to the same cluster structure.
- the particle produced a track segment at least in the N_{layer} first layers and a seed object is found within a distance $\Delta_{(track-cluster)_1}$ to the track projection. Since only a cluster starting with a track segment has to be associated, an additional distance cut $\Delta_{(track-cluster)_2}$ between seed objects and the track projection is applied. This decreases the confusion for small separation distances between nearby particles. The same track-to-cluster association and cluster merging is then performed as above.

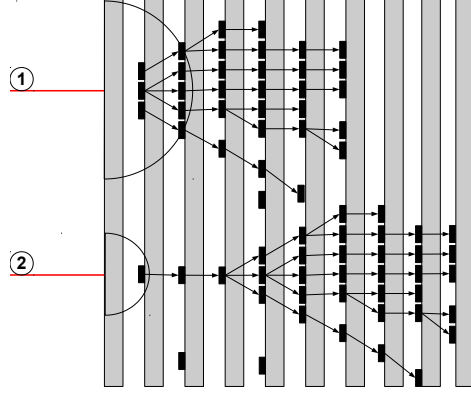


Figure 5: Schematic view of the energy driven track cluster algorithm.

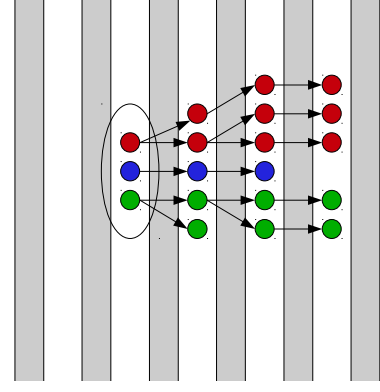


Figure 6: Schematic view of the neutral tree merging algorithm.

Figure 5 shows a schematic view of the two different scenarios. The upper one corresponds to the case where an early interaction is found, and the lower one where a primary track segment of a cluster is found.

Neutral tree merging This algorithm is designed for neutral particle interactions for which the first interacting layer contains a few seeds. Figure 6 shows a configuration in which three trees have been built (with three colours) for one neutral particle interaction. We can see that the seeds in the first interacting layer all belong to the same cluster. We group all the tree seeds within the same layer and at maximum distance of Δ_{seed} . Then all of these trees are merged in the cluster.

Pointing cluster association This step aims at associating neutral fragments (daughter cluster) to other fragments which may be charged or neutral clusters (parent clusters). We start by identifying the clusters that have at least $N_{objects}$ objects in at least N_{layer} contiguous layers. The selected cluster could be either a parent or a daughter cluster. Then we proceed as follows :

1. A linear 3D straight line fit is performed over the position of all the hits of each cluster (without weights). This defines the axis of each cluster.
2. The clusters are sorted by their most downstream layers (most downstream hit in the cluster) l_{inner} .
3. Starting from the most downstream cluster i , we look for a parent cluster j for which $l_{inner,i} > l_{inner,j}$.
4. Among these candidate parent clusters, we look for those for which $d_{proj} < d_{proj,cut}$ and $\theta_{i,j} < \theta_{i,j,cut}$ where :
 - d_{proj} is the distance between the candidate daughter cluster axis and the candidate parent cluster barycentre (line-to-point distance)
 - $\theta_{i,j}$ is the angle between the axis of the two clusters
and we choose the cluster for which d_{proj} is minimal.
5. Among this same list of candidate parent clusters, we look for those satisfying the condition $d_{cross} < d_{cross,cut}$ and $d_{closest} < d_{closest,cut}$ where :

- d_{cross} is the distance at closest approach (d.c.a) between the two cluster axes
- $d_{closest,i,j}$ is the closest distance between an object of the parent cluster and the point of closest approach of the cluster axes (distance at closest approach)

and we choose the cluster for which d_{cross} is minimal.

6. We choose the best candidate parent cluster among the two previous methods above. Many cases may happen i) no parent cluster is found, then no parent cluster is assigned to this daughter cluster, ii) one of the two methods has found a parent cluster or the two methods provide the same parent, then we assign it to the daughter cluster, iii) the two methods have found a parent cluster but there are not the same one. In this case the closest candidate parent cluster among the two in terms of barycentre distance is assigned to the daughter cluster.

7. If no parent cluster has been found for a cluster, stop processing this cluster, else :

8. If the parent cluster has no associated track, merge the two clusters, else :

9. We define the variable Ψ as :

$$\Psi = \left| \frac{p - E_{tot}}{f_{res} \cdot \sigma_E \cdot p} \right| \quad (3.3)$$

where :

- p is the track momentum of the parent cluster
- E_{tot} is the total energy estimated from the combined hit list of the parent and daughter clusters
- σ_E is the calorimeter energy resolution at the track momentum p
- f_{res} is a multiplicative factor⁴

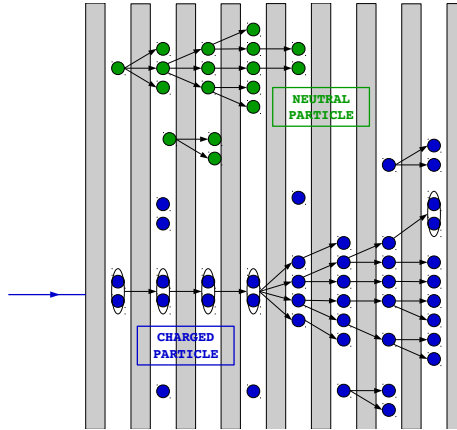


Figure 7: Schematic view of the final ArborPFA output

⁴The parameter f_{res} is used to reduce or enlarge the accepted range of the difference $p - E_{tot}$. A higher value of this parameter will accept a merging with a higher difference $p - E_{tot}$.

239 We check then that the Ψ defined for the parent and daughter clusters is less than Ψ_{cut} and
240 if the difference between p and E_{tot} after the cluster merging (parent + daughter clusters)
241 decreases. The two clusters are merged if the previous conditions are satisfied.

242 **Small neutral fragment merging** At this stage, the main part of the shower of each particles has
243 been identified. Only isolated objects and small tree structures that surround the showers are not
244 associated. First, these small structures are identified if their size is less than N_{cut} objects. Then
245 for all showers and small structures, the barycentre is computed and each small structure is merged
246 within the shower that has the smallest distance between barycentres.

247 **Particle flow object creation** Particle flow objects are built from the produced clusters after all
248 the steps described above (Figure 7). Charged PFOs are built from clusters that have an associated
249 track, while other clusters are considered as neutral PFOs.

4. Single particle study

4.1 Setup

To study the single particle performance of the algorithm, we use the SDHCAL charged pion data taken at CERN on the H6 line of SPS in 2012 from 10 GeV up to 80 GeV. The list of runs for the different energies can be found in Appendix B. In order to select only pions, an event selection is performed as described in [1].

To correctly emulate a charged pion for the reconstruction program, a fake track is created in front of the calorimeter. A global barycentre of all hit positions in the transverse plane (x and y axes) is calculated. A new barycentre is then calculated using only hits in the 4 first layers and within a region of 8x8 cells around the global barycentre in the x and y directions. This defines the shower entering point in the first layer. From the entering point of the shower, a straight track is created along the beam axis (z direction) with momentum equal to that of beams.

The calorimeter hits and the created track are then loaded into the PandoraSDK toolkit [6] within a single hcal endcap geometry (no magnetic field) and processed by the ArborPFA algorithms. An event display of a single pion event is shown on figure 8.

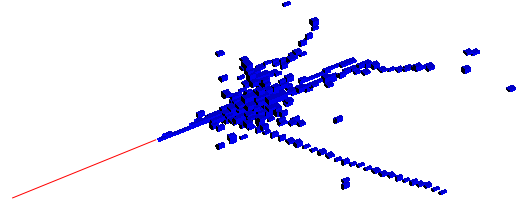


Figure 8: Event display of a 50 GeV pion shower in the SDHCAL detector

4.2 Single particle analysis

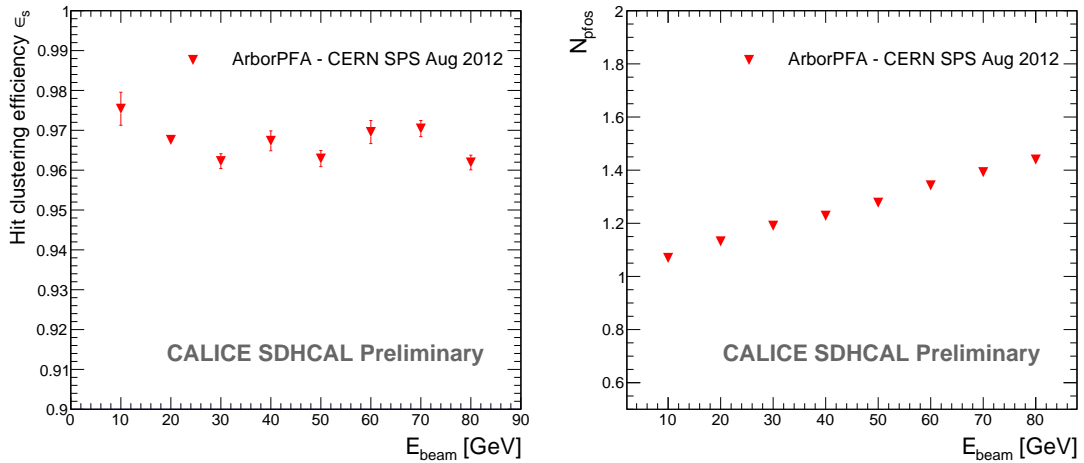


Figure 9: Hit clustering efficiency (left) and the mean number of reconstructed particles (right) after ArborPFA reconstruction on single pion shower events with the SDHCAL prototype

273 We define the efficiency of the single particle reconstruction, or the hit clustering efficiency
 274 ϵ_s as the number of hits recovered by the ArborPFA program and correctly attached to track in
 275 front of the calorimeter. Figure 9 shows the mean efficiency of the single particle reconstruction
 276 (left) and the mean number of reconstructed particles (right) as a function of the beam energy after
 277 applying ArborPFA. It shows a constant efficiency of over 96% over the whole beam energy range.
 278 Since the number of hits increases with the energy, the number of missed hits in the reconstructed
 279 charged particle also increases. Consequently, the mean number of reconstructed particles shows
 280 an increase which is directly due to shower splitting. This number grows up to 1.45 particles at
 281 80 GeV but has only a small impact on the reconstructed energy and energy resolution because
 282 the small additional clusters represent a small amount of energy. Indeed, figure 10 shows the
 283 reconstructed energy and energy resolution of a single charged pion before and after running the
 284 ArborPFA program.

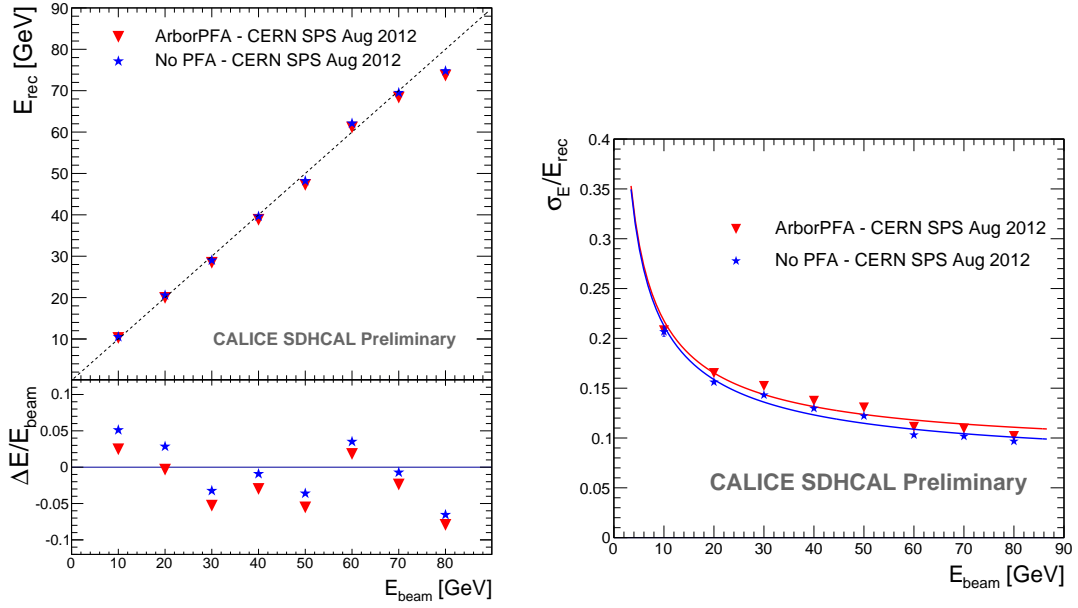


Figure 10: Reconstructed energy (left) and energy resolution (right) before (blue) and after (red) ArborPFA reconstruction on single pion shower event with the SDHCAL prototype

285 The linearity is shown below the reconstructed energy and is defined as :

$$\Delta E/E_{beam} = (E_{rec} - E_{beam})/E_{beam} \quad (4.1)$$

286 These energy points are extracted using two fits of the energy distributions : i) a gaussian
 287 distribution fit over the full reconstructed distribution is first performed. The mean $\mu_{E,first}$ and
 288 width $\sigma_{E,first}$ are extracted, and ii) a second gaussian fit is then performed over the range $[\mu_{E,first} - 1.5 \cdot \sigma_{E,first} ; \mu_{E,first} + 1.5 \cdot \sigma_{E,first}]$. From the latter, we extract the final values of the reconstructed
 289 energy and energy resolution defined as the mean μ_E and the width σ_E respectively of the gaussian
 290 fit (same procedure applied in [1]). The efficiency plot has shown that some hits are missing
 291 after reconstruction so it is expected to have a small energy decrease in the reconstructed energy.
 292

293 Nevertheless, the linearity is still within 8% as before applying the reconstruction. The energy
294 resolution is also not so much affected after reconstruction.

5. Separation of two close-by hadronic showers

The ability of a particle flow algorithm to disentangle close-by showers is a key point for the reconstruction in detectors such as ILD of the ILC. To study the confusion between neutral and charged hadrons and the ability of the ArborPFA algorithm to disentangle them, we again use the same test beam data of the SDHCAL prototype. Two different pion showers are first overlaid in the same event and the ArborPFA algorithm is run on the overlaid event with the same parameters as for the single particle study. An analysis of the separation is then performed in order to extract the performance of the algorithm.

5.1 Overlay procedure and setup

In order to study the separation of nearby hadronic showers, two events from test beam data are overlaid in one event. We have chosen to overlay 10 GeV pions and pions with different energies from 10 GeV up to 50 GeV by step of 10 GeV. Different separation distances between the shower entry point from 5 cm up to 30 cm by step of 5 cm were used. The choice of this energy range is motivated by the fact that it is the typical single particle energies foreseen at the ILC within jets [3].

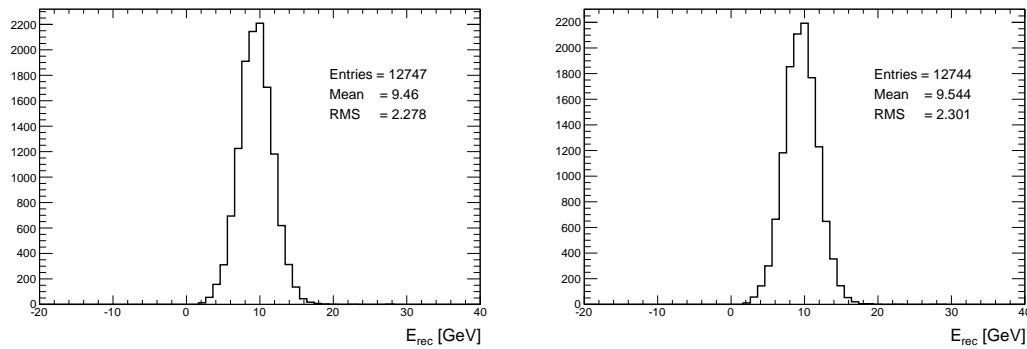


Figure 11: The reconstructed energy of the 10 GeV neutral hadron after the overlay procedure with a 50 GeV charged hadron with a separation distance of 30 cm (left) and 5 cm (right)

The overlay event algorithm is processed as follow :

1. The entering track segments of the two showers are determined as for the single particle case. This allows to identify the shower entering points and starting points.
2. For one of the two pion showers, the hits belonging to its track segments, if any, are removed from the event in order to emulate a neutral hadron shower.
3. The two showers are then centred along the X and Y axis at the center of the calorimeter. No shift is performed on the Z direction (beam line).
4. The showers are then shifted along the X axis by a distance of $-d/2$ for the neutral hadron and $+d/2$ for the charged particle.

- 319 5. The two events are then overlaid in a new one. At this step a problem may occur : while
 320 mixing the showers in the event, pair of hits may overlap in the same cell. Knowing that we
 321 are using a semi digital readout and that the information of the deposit charge in each cell
 322 is not available in the data, we need to assign a new threshold by using an approximation.
 323 The most intuitive one is to keep the highest threshold of the two hits. Figure 11 shows the
 324 reconstructed energy of the 10 GeV neutral hadron overlaid with a 50 GeV charged hadron
 325 at 30 cm distance (left) and 5 cm distance (right). The latter case is the worst one that can
 326 appears in this study given the energy points and the distances we have chosen. By comparing
 327 the two plots, we can see that the effect of this approximation on the reconstructed energy is
 328 negligible.
- 329 6. The hits are tagged with respect to our initial showers. All the hits of the neutral hadron are
 330 tagged 1 while for the charged hadron the hits are tagged 2. The overlaid hits are tagged 3 so
 331 that the information on the overlaid hits can be retrieved after reconstruction.
- 332 7. A new event is created containing the overlaid showers and the entering point of the charged
 333 particle track after shifting as shown on figure 12.

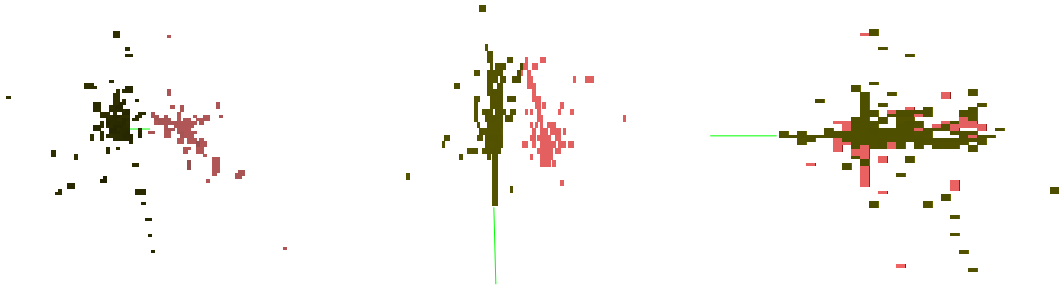


Figure 12: Event display of a 10 GeV neutral hadron overlaid with a 30 GeV charged hadron at 20 cm separation distance on three different views (XoY on left, XoZ in center and YoZ on right). Colours correspond to the reconstructed PFOs after running the ArborPFA program. The green straight line is the track generated in front of the calorimeter.

334 5.2 Overlaid particles analysis

335 Figure 13 shows the mean number of PFOs after running the ArborPFA program on a 10 GeV neu-
 336 tral hadron overlaid with a charged hadron at different energies and different separation distances
 337 between them. The behaviour at a large separation distances where the number of PFOs increases
 338 with the charged particle energy matches the behaviour of the number of PFOs in the single particle
 339 study. We can also see that the sum of the number of PFOs for the single particle is compatible
 340 with the number of PFOs for the overlay. The mean number of PFOs is stable at large separation
 341 distances but decreases for distances shorter than 10 cm from 2.1 PFOs down to 1.8 PFOs due to
 342 the showers overlap and confusions.

343 To quantify the separation, we define the efficiency and the purity related to the reconstruction
 344 of one of the two related showers as :

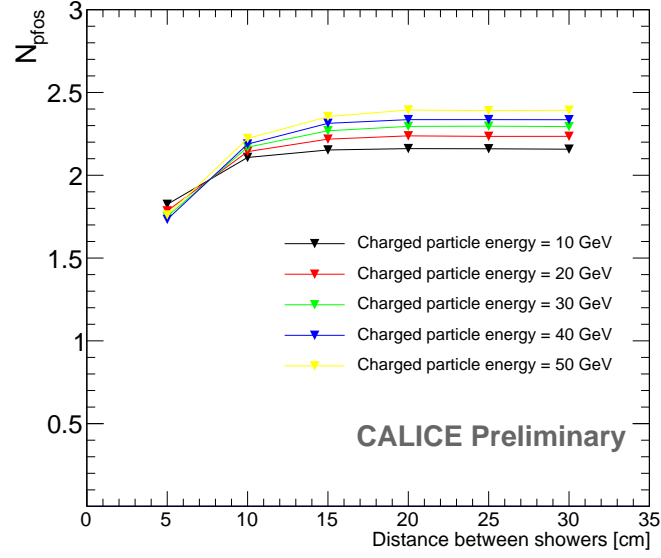


Figure 13: The mean number of PFOs after running the ArborPFA program on overlaid particles.

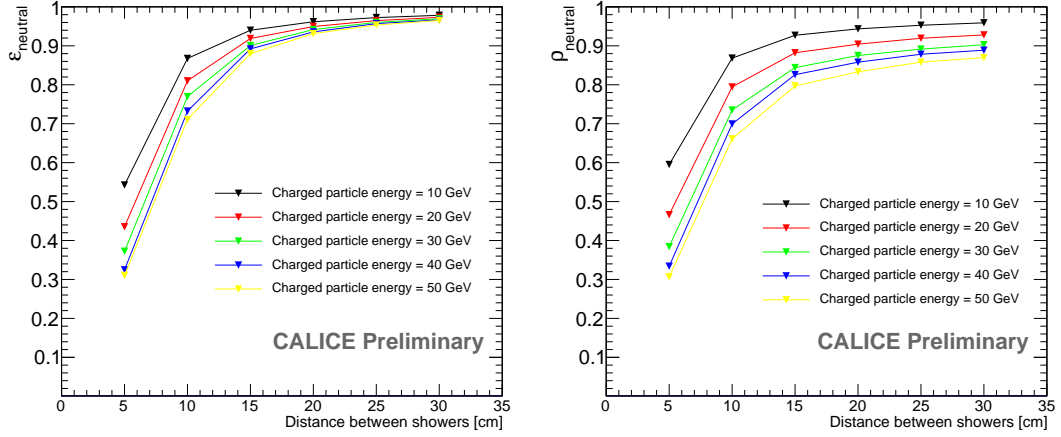


Figure 14: The efficiency (left) and purity (right) of the 10 GeV neutral hadron after separation with a charged hadron

$$\varepsilon = \frac{N_{hit_{good}}}{N_{hit_{ini,tot}}} \quad (5.1)$$

$$\rho = \frac{N_{hit_{good}}}{N_{hit_{rec,tot}}} \quad (5.2)$$

with $N_{hit_{good}}$ the number of hits that initially belong to the particle and correctly assigned after reconstruction, $N_{hit_{rec,tot}}$ the total number of hits of the reconstructed shower and $N_{hit_{ini,tot}}$ the total number of hits of the particle before reconstruction.

Figure 14 shows the efficiency (left) and the purity (right) of the neutral hadron for different charged particle energies and different separation distances. In the same way as for the mean number of PFOs, at small distances the two showers start to overlap and confusions appear while the reconstruction is performed. Thus, some hits of the neutral hadron are assigned to the charged one (and vice versa) and the efficiency and purity decrease. At large separation distances, the purity does not tend to 100%. This is due to the last performed algorithm (small neutral fragment algorithm) which tends to merge the small neutral cluster fragments in their closest parent cluster, without taking care of the parent cluster size or energy. Since the number of neutral fragments for a single hadron particle increases with the energy, a non-negligible part of the charged hits is assigned to the neutral hadron, leading to a decrease of its purity.

Figure 15 (on the left) shows the fraction of events where at least one neutral hadron has been reconstructed. As expected, the number of reconstructed neutral particles decreases with the separation distance. From 30 cm down to 15 cm, this fraction is stable and very closed to 100%. At 10 cm, confusions start appearing and the neutral hadron is sometimes merged in the charged one, leading to a small decrease of this fraction. At 5 cm, we can see that the fraction strongly depends on the charged particle energy and goes from 73% of reconstructed events for the 10 GeV charged particle case down to 60% for the 50 GeV charged particle case.

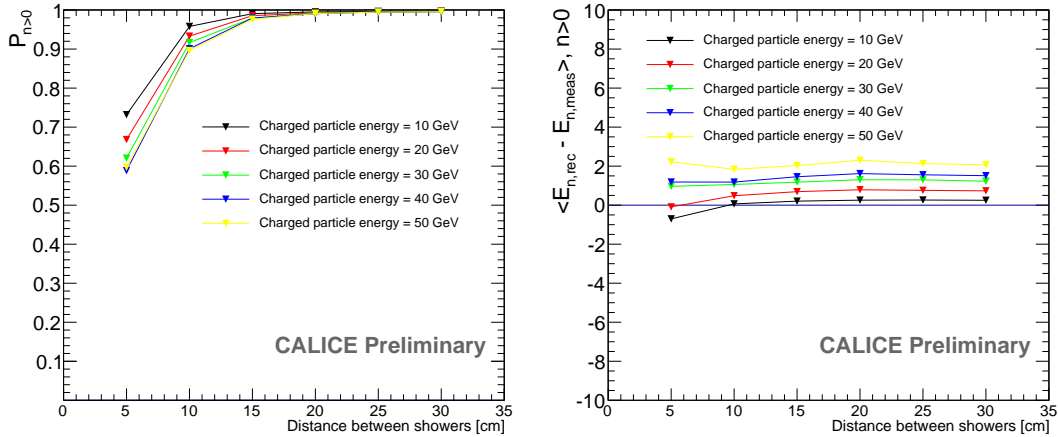


Figure 15: Left : The fraction of events where at least one neutral hadron has been reconstructed.
Right : The same variable when at least one neutral hadron has been reconstructed.

Figure 15 (on the right) shows the mean difference between the reconstructed energy and the measured energy of the neutral hadron in the case where at least one neutral hadron has been reconstructed. In the same way as for the purity, the reconstructed energy of the neutral hadron increases with the charged particle energy. This plot also shows a constant evolution of the reconstructed energy with the separation distance. This means that the reconstruction of the neutral hadron at very small distance (5 cm) has a *binary-like* behaviour, either well reconstructed or completely merged in the charged hadron.

6. Summary

The ArborPFA algorithm has been described in details with all the sub-algorithms.

A single particle study has been performed on SDHCAL test beam data taken at SPS at CERN during August and September 2012 [1]. Single pion showers have been selected and a track in front of the calorimeter has been created in order to emulate a TPC track.

The results showed a good efficiency with more than 95% of hits assigned to the reconstructed charged particle over the whole energy range. The mean number of PFOs shows an increase with the energy from 1.1 PFOs at 10GeV up to 1.4 PFOs at 80 GeV growing linearly. The reconstructed energy of the single charged hadron is close to the one applied before running the algorithm with a small decrease due to the 5% of inefficiency and thus the energy resolution increases too.

The algorithm has also been applied in order to separate close-by hadronic showers. Two different charged hadron showers with different energies from the same test beam data set have been overlaid in the same event with different separation distances. For one of the two showers the mip track inside the calorimeter has been identified and removed from the event in order to emulate a neutral hadron particle. For the other particle, a track has been generated in front of the calorimeter and pointing on the particle entry point, as for the single particle case.

The results showed a good neutral hadron efficiency and purity until 10 cm separation distance where a non negligible confusion starts to appear.

The difference between the reconstructed energy and the measured energy of the neutral hadron in the case where at least one neutral hadron has been reconstructed showed an increase with the charged hadron energy for all the separation distances due to the small neutral fragment merging algorithm. At small separation distance (5cm), the difference stays constant and shows that the neutral hadron reconstruction has a *binary-like* behaviour, either a very good reconstruction or merged in the charged hadron.

This work will be extended shortly to include the electromagnetic calorimeter as well as the other sub-detectors in the framework of the ILD detector with the aim to separate charged and neutral hadrons produced in jets to improve on the PFA performances.

400 **References**

- 401 [1] Calice Collaboration, *First results of the CALICE SDHCAL technological prototype*, CAN-037
- 402 [2] J. Carwardine *et al.*, *International Linear Collider Technical Design Report*. 1) Executive Summary, 2)
- 403 Physics, 3) Accelerator, 4) Detectors. 12 June 2013
- 404 [3] O. Lobban, A. Sriharan, R. Wigmans, *On the energy measurement of hadron jets*, *Nucl. Instrum. Meth.*
- 405 **A495** (2002) 107-120
- 406 [4] F. Gaede, Marlin and LCCD: Software tools for the ILC, *Nucl.Instrum.Meth.* A559 (2006) 177-180
- 407 [5] M. A. Thomson, *Particle Flow Calorimetry and the PandoraPFA Algorithm*,
- 408 `phys.int-det/0907.3577`
- 409 [6] J. S. Marshall, M. A. Thomson, *The Pandora Software Development Kit for Pattern Recognition*,
- 410 `phys.int-det/1506.05348`
- 411 [7] M. Ruan, *Arbor, a new approach of the Particle Flow Algorithm*, Proceeding of CHEF 2013.
- 412 `hep-ex/1403.4784`
- 413 [8] ILCsoft, 2012. <http://ilcsoft.desy.de/portal>
- 414 [9] ROOT, 1995-2015, <https://root.cern.ch/drupal>

415 **A. ArborPFA algorithm parameters**

416 **Object creation algorithm**

Parameter name	value
MaxClusterSize	4
IntraLayerDistance	11 mm

- 417 • MaxClusterSize
418 → The maximum intra layer cluster size to build an object with. Else the object is split in
419 single calo hit objects
- 420 • IntraLayerDistance
421 → The nearest neighbour intra layer clustering maximum distance

422 **Track segment candidate tagging algorithm**

Parameter name	value
MaxNNeighbors	6
IntraLayerNeighbourDistance (Δ_{mip})	50 mm

- 423 • MaxNNeighbors
424 → The maximum number of neighbouring objects within a layer
- 425 • IntraLayerNeighbourDistance (Δ_{mip})
426 → The maximum distance between two neighbours in a layer used for the neighbour count-
427 ing

428 **Primary track connection**

Parameter name	value
ConnectionDistance	110 mm
BackwardConnectorWeight	2
ForwardConnectorWeight	3
OrderParameterAnglePower	1
OrderParameterDistancePower	5
MaxNEmptyConsecutiveLayers	3

- 429 • ConnectionDistance
 430 → The maximum connection distance used for the primary track connectors creation
- 431 • BackwardConnectorWeight
 432 → The backward connector weight assigned for the reference vector computation
- 433 • ForwardConnectorWeight
 434 → The forward connector weight assigned for the reference vector computation
- 435 • OrderParameterAnglePower
 436 → The angle power parameter of the κ parameter while cleaning connectors
- 437 • OrderParameterDistancePower
 438 → The distance power parameter of the κ parameter while cleaning connectors
- 439 • MaxNEmptyConsecutiveLayers
 440 → The maximum consecutive empty layers to take into account for the connector seeding

441 **Connector seeding 1**

Parameter name	value
ConnectionDistance	45 mm

- 442 • ConnectionDistance
 443 → The maximum connection distance used for a connector creation

444 Connector cleaning 1

Parameter name	value
BackwardConnectorWeight	2
ForwardConnectorWeight	2
OrderParameterAnglePower	1
OrderParameterDistancePower	5
ReferenceDirectionDepth	1

- 445 • BackwardConnectorWeight
- 446 → The weight of a backward connector assigned in the reference direction vector calculation.
- 447 • ForwardConnectorWeight
- 448 → The weight of a forward connector assigned in the reference direction vector calculation.
- 449 • OrderParameterAnglePower
- 450 → The θ angle power parameter used for the κ parameter computation
- 451 • OrderParameterDistancePower
- 452 → The Δ distance power parameter used for the κ parameter computation
- 453 • ReferenceDirectionDepth
- 454 → The forward connector depth used for the reference vector computation

455 Connector seeding 2

Parameter name	value
ConnectionDistance	65 mm
ConnectionAngle	0.7 rad

- 456 • ConnectionDistance
- 457 → The maximum connection distance used for a connector creation
- 458 • ConnectionAngle
- 459 → The maximum angle between two connectors

460 Connector cleaning 2

Parameter name	value
BackwardConnectorWeight	0.1
ForwardConnectorWeight	5
OrderParameterAnglePower	1
OrderParameterDistancePower	5
ReferenceDirectionDepth	2

- 461 • BackwardConnectorWeight
462 → The weight of a backward connector assigned in the reference direction vector calculation.
- 463 • ForwardConnectorWeight
464 → The weight of a forward connector assigned in the reference direction vector calculation.
- 465 • OrderParameterAnglePower
466 → The θ angle power parameter used for the κ parameter computation
- 467 • OrderParameterDistancePower
468 → The Δ distance power parameter used for the κ parameter computation
- 469 • ReferenceDirectionDepth
470 → The forward connector depth used for the reference vector computation

471 Energy driven track cluster association

Parameter name	value
TrackToClusterDistanceCut1	75 mm
TrackToClusterDistanceCut2	55 mm
FirstInteractingLayerNSeedCut	15
TrackToClusterNLayersCut	3
TrackClusterPsi2Cut	3
Psi2SigmaFactor	1.5

- 472 • TrackToClusterDistanceCut1
473 → The maximum distance between the track projection at calorimeter front face and a cluster
474 seed. This distance is used to detect an early interacting cluster.
- 475 • TrackToClusterDistanceCut2
476 → The reduced maximum distance between the track projection at calorimeter front face and
477 a cluster seed. This distance is used when no early interacting cluster has been detected.

- 478 • FirstInteractingLayerNSeedCut
479 → The cut on the number of cluster seeds found within a the distance TrackToClusterDis-
480 tanceCut1 to detect an early cluster interaction.
- 481 • TrackToClusterNLayersCut
482 → The number of inner layers to look for cluster seeds to associate.
- 483 • TrackClusterPsi2Cut
484 → The ψ^2 cut applied while associating clusters to a track.
- 485 • Psi2SigmaFactor
486 → The f_{res} factor on denominator used to compute the ψ^2 for track-to-cluster compatibility
487 (see equation 3.3)

488 Neutral tree merging

Parameter name	value
SeedSeparationMerge (Δ_{seed})	25 mm

- 489 • SeedSeparationMerge (Δ_{seed})
490 → The maximum distance between two cluster seeds within a layer to perform a cluster
491 merging

492 Pointing cluster association

Parameter name	value
MinNObjects	4
MinNLayers	4
FitToBarycentreDistanceCut	30 mm
FitToBarycentreAngleCut	$\frac{\pi}{6}$ rad
FitToFitDistanceCut	20 mm
FitDistanceApproachCut	20 mm
Chi2NSigmaFactor	1.5
Chi2AssociationCut	1

- 493 • MinNObjects
494 → The minimum number of objects within a cluster in order to to be candidate for the
495 pointing cluster association
- 496 • MinNLayers
497 → The minimum number of layers within a cluster (outermost - innermost + 1) in order to
498 be candidate for the pointing cluster association

- 499 • FitToBarycentreDistanceCut
500 → The cut applied on the distance between the daughter cluster fit and the parent cluster
501 barycentre position (point-to-line distance)
- 502 • FitToBarycentreAngleCut
503 → The cut applied on the angle between the daughter and parent cluster fits
- 504 • FitToFitDistanceCut
505 → The cut applied on the distance between the daughter and parent cluster fits (line-to-line
506 distance)
- 507 • FitDistanceApproachCut
508 → The cut applied on the closest distance between a parent cluster object and the daughter
509 cluster crossing point at the parent and daughter cluster fit closest approach.
- 510 • Chi2NSigmaFactor
511 → The N_{res} factor on denominator used to compute the χ^2 for track-to-cluster compatibility
512 (see equation 3.3) using the merged cluster (daughter + parent)
- 513 • Chi2AssociationCut
514 → The χ^2 cut applied on the merged clusters compatibility with a track when associating a
515 neutral daughter cluster with a charged parent cluster.

516 **Small neutral fragment merging**

Parameter name	value
MaximumDaughterNObject	20
LargeDistanceCut	1000 mm

- 517 • MaximumDaughterNObject
518 → The maximum number of objects to consider the cluster as a small neutral fragment to
519 merge it into a bigger parent cluster
- 520 • LargeDistanceCut
521 → The maximum distance between a small neutral fragment and a potential parent cluster

522 **B. SDHCAL data**

Energy	10 GeV	20 GeV	30 GeV	40 GeV	50 GeV	60 GeV	70 GeV	80 GeV
Run number	715693	715675	715747	715748	715751	715753	715754	715756

Figure 16: List of SDHCAL pion runs used for reconstruction

523